Pole Rebalancing Methods for Pole-to-ground Faults in Symmetrical Monopolar HVDC Grids

Mian Wang, *Student Member, IEEE,* Willem Leterme, *Member, IEEE,* Geraint Chaffey, *Member, IEEE,* Jef Beerten, *Member, IEEE,* and Dirk Van Hertem, *Senior Member, IEEE*

***Abstract*—Pole rebalancing in symmetrical monopolar HVDC grids is necessary to remove pole imbalances resulting from pole-to-ground faults. For selective protection employing DC circuit breakers, the interaction between DC circuit breakers and pole rebalancing methods have not been studied. This paper proposes new strategies for pole rebalancing methods to deal with DC circuit breaker operation in HVDC grids. A complete analysis of pole rebalancing using equipment at DC or AC side is performed for all stages of the fault clearing process. Based on the analysis, new control strategies are proposed to optimize the use of the pole rebalancing equipment. The proposed control methods are shown to enable the pole rebalancing equipment to meet the required high protection speed and low losses. Both DC and AC side equipment such as dynamic braking systems and AC groundings are investigated and proven to be applicable for pole rebalancing in selective protection strategies. The impact of the breaker technology on the interaction between DC circuit breaker requirements and pole rebalancing needs is investigated in detail. The conclusions are validated using EMTP simulation on a four terminal test grid.**

***Index Terms*—Pole rebalancing, dynamic braking system, AC side grounding, symmetrical monopole, HVDC grid protection.**

I. Introduction

VOLTAGE source converter (VSC) based high voltage direct current (HVDC) grids are a key solution to integrate massive amounts of renewable energy and provide the increased reliability and flexibility required to handle the variable nature of renewable sources. However, to achieve high reliability, HVDC grid protection system is essential, yet challenging due to the nature of the DC fault behaviour [1]. At present, the majority of VSC-HVDC systems are point-to-point links in a symmetrical monopolar configuration. Interconnecting such links could be a cost effective solution, making symmetrical monopolar configuration a viable option for the future HVDC grids [1].

Various protection strategies have been proposed and are broadly classified as selective, partially-selective and non-selective [2]. Selective strategies are highly advantageous since they minimize the DC fault impact by protecting each component individually using DC circuit breakers. Numerous DC circuit breaker technologies have been proposed to tackle the challenge of interrupting a DC fault current, such as resonance mechanical and hybrid breakers [3], [4]. DC circuit breaker technologies and breaker opening times have been summarized in [5], [6]. The breaker opening time is in the order of few ms for hybrid breakers, and 10 ms to 20 ms for active and passive resonance mechanical breakers. Inductors are typically used in series with the DC circuit breakers to limit the rate-of-rise of the fault current [7].

Pole-to-ground faults in symmetrical monopolar systems result in persistent overvoltage on the healthy pole, and consequently, pole rebalancing is a necessary step to restore the system. Most literature have focused on DC faults in low impedance grounded grids as these fault conditions entail the most stringent requirement on the breaking current [8]–[10]. By contrast, pole-to-ground faults in symmetrical monopolar systems have not received attention to the same extent. In addition, unlike present practice in AC protection, DC circuit breakers might not be used to interrupt currents associated with all faults, resulting in the possibility to reduce the overall cost of the HVDC grid protection [11]. For instance, if the DC circuit breakers are designed for breaking the currents associated with pole-to-ground rather than pole-to-pole faults, their required current interruption and energy absorption capabilities can be decreased. In such cases, additional measures are needed to deal with pole-to-pole faults, for example, using AC circuit breakers to interrupt the fault current, thus accepting a total DC system disconnection in case a pole-to-pole fault occurs, and auxiliary equipment to protect the DC circuit breakers in case they cannot withstand the fault currents.

Up to now, for selective protection employing DC circuit breakers, the interaction between DC circuit breakers and pole rebalancing methods have not been studied. In the literature, the methods for pole rebalancing are mainly studied in HVDC grids without DC circuit breakers. These methods use a dynamic braking system (DBS) or an AC side grounding permitting zero sequence currents [12], [13]. However, these methods do not deal with coordination between breaker operation and pole rebalancing. Evidence towards the efficacy of using a DBS for pole rebalancing with DC circuit breakers has only been briefly presented in [14]. As future HVDC grids are likely to be provided by multiple vendors, an in-depth understanding of the interaction between various pole rebalancing methods and breaker technologies is crucial to design effective HVDC grid protection at the system level.

The main contribution of this paper is to provide new strategies for pole rebalancing methods to deal with DC circuit breaker operation in HVDC grids. An in-depth analysis

This project has received funding from the European Unions Horizon 2020 research and innovation programme under grant agreement No. 691714. The work of Jef Beerten is funded by a research grant of the Research Foundation-Flanders (FWO). The authors would like to thank the following partners in PROMOTioN project for their input and feedback, Ilka Jahn and Niklas Svensson.

The authors are with EnergyVille/Electa Research Group, Electrical Engineering Department ESAT, KU Leuven, 3001 Heverlee, Belgium. (e-mail: mian.wang@kuleuven.be).

of pole rebalancing method is performed to identify their interaction with DC circuit breakers. For the first time, a complete analysis of pole rebalancing is done for all stages of the fault clearing process for selective protection strategies. Based on the analysis, new control strategies are proposed to effectively use pole rebalancing equipment in conjunction with DC circuit breakers. In addition, the impact of the DC circuit breaker technology on the required ratings for pole rebalancing equipment and surge arresters is investigated in an HVDC grid setting to optimize key parameters for pole rebalancing in selective protection strategies.

This paper is structured as follows: Section II investigates the pole-to-ground fault behaviour, and presents the pole rebalancing principle and potential candidate equipment. Section III presents the proposed control strategies for the DBS and AC groundings. Section IV introduces a four terminal HVDC test grid and its main parameters. Section V first investigates the applicability of various pole rebalancing equipment at DC and AC sides for selective protection strategies, and then analyses the interaction between the requirements on the DC circuit breaker and pole rebalancing equipment. Finally, conclusions are drawn in Section VI.

II. Pole-to-ground Faults and Pole Rebalancing Principle

A. Pole-to-ground Fault Behaviour

The pole-to-ground fault behaviour can be explained using a zero sequence equivalent circuit, adopting common and differential mode definitions as introduced in [15], [16]. These definitions are recapitulated in (1) and (2) using notations indicated in Fig. 1 (a).

$$u_\phi^\Delta = \frac{u_\phi^L - u_\phi^U}{2}, \quad u_\phi^\Sigma = u_\phi^U + u_\phi^L \tag{1}$$

$$i_\phi^\Delta = i_\phi^U - i_\phi^L, \quad i_\phi^\Sigma = \frac{i_\phi^U + i_\phi^L}{2}, \tag{2}$$

where ϕ represents the phase a, b, or c; u_ϕ^L, u_ϕ^U are the voltages across the lower and upper arm submodules; and i_ϕ^L, i_ϕ^U are the lower and upper arm currents. The differential and common mode voltages can be expressed as

$$u_\phi^s = \frac{u_{DCp} - u_{DCn}}{2} + u_\phi^\Delta - \frac{sL_{arm}}{2} i_\phi^\Delta \tag{3}$$

$$u_\phi^\Sigma + 2sL_{arm} i_\phi^\Sigma = u_{DCp} + u_{DCn}. \tag{4}$$

where u_{DCp} and u_{DCn} are the positive and negative pole-to-ground voltages. Applying Park's transformation to (3) and (4),

$$\begin{bmatrix} u_0^s \\ u_{d,q}^s \end{bmatrix} = \begin{bmatrix} \frac{u_{DCp} - u_{DCn}}{2} + u_0^\Delta - \frac{sL_{arm}}{2} i_0^\Delta \\ u_{d,q}^\Delta - \frac{sL_{arm}}{2} i_{d,q}^\Delta \end{bmatrix} \tag{5}$$

$$\begin{bmatrix} u_0^\Sigma \\ u_{d,q}^\Sigma \end{bmatrix} = \begin{bmatrix} u_{DCp} + u_{DCn} - 2sL_{arm} i_0^\Sigma \\ -2sL_{arm} i_{d,q}^\Sigma \end{bmatrix}. \tag{6}$$

The equivalent circuit of the DC side described by the zero sequence of (6) is depicted in Fig. 1 (b), where u_0^Σ is split to the sum voltages of the upper and lower arm,

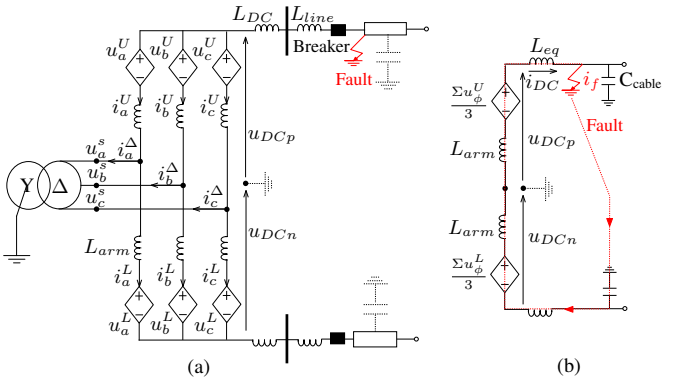

Figure 1. Multilevel modular converter (MMC) station with symmetrical monopolar configuration: (a) Schematic diagram (b) Zero sequence equivalent circuit (L_{eq} includes the DC smoothing reactor and the series line inductor).

$\Sigma u_\phi^U/3$ and $\Sigma u_\phi^U/3$. During a pole-to-ground fault, a sudden drop of u_{DCp} results in the faulted pole and healthy pole discharging and charging, respectively. Once the faulted pole is fully discharged, the DC current i_{DC} decays to zero or the pre-fault steady-state value depending whether the converter continues operating or blocks as self-protection. The steady-state healthy pole voltage is the pole-to-pole DC voltage if the converter continues operating. If AC grounding is not present, the zero sequence current i_0^Δ is zero, and the converter AC voltage u_0^s shifts from zero to minus pole-to-ground DC voltage during a solid pole-to-ground fault according to (5).

B. Operating Principle of Pole Rebalancing

Pole rebalancing in symmetrical monopolar configuration is essentially achieved by providing a discharge path for the healthy pole. This discharge path can be provided either at the DC or AC side, by a DBS or an AC grounding as shown in Fig. 2 and Fig. 3.

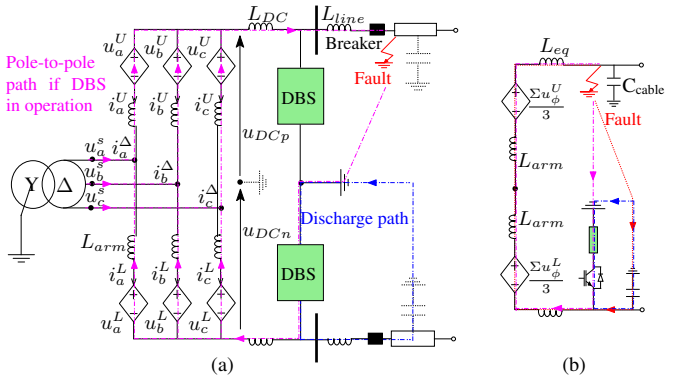

Figure 2. Fault path and pole rebalancing path with DBS (a) Schematic diagram (b) Zero sequence equivalent circuit.

Pole rebalancing equipment at the DC and AC side is shown in Fig. 4 and Fig. 5, respectively. Potential candidates for the DBS circuits include conventional DBS circuit for offshore wind application using lumped braking resistor (R_{DBS}), and alternative DBS circuits using surge arresters [17]–[19]. The surge arresters of these alternative DBS circuits differ from

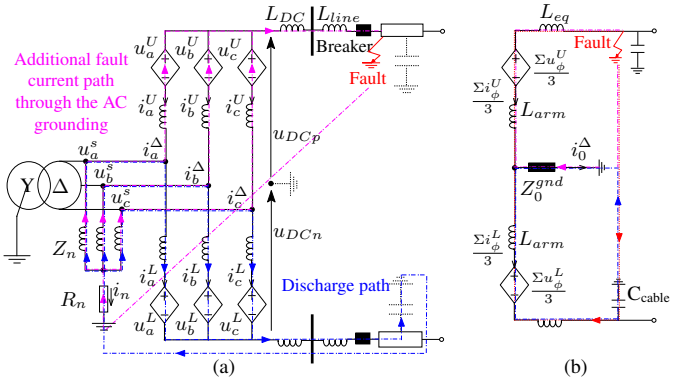

Figure 3. Fault path and pole rebalancing path with AC grounding (a) Schematic diagram (b) Zero sequence equivalent circuit.

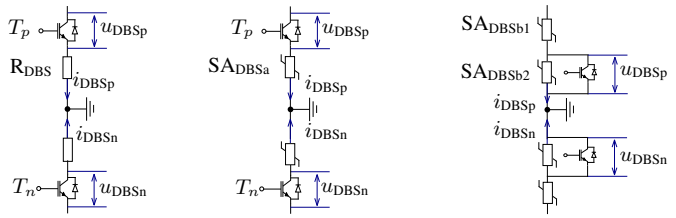

Figure 4. DC side pole rebalancing potential candidates (a) DBS circuit 1: lumped braking resistor based DBS (b) DBS circuit 2: surge arrester based DBS (c) DBS circuit 3: surge arrester based DBS.

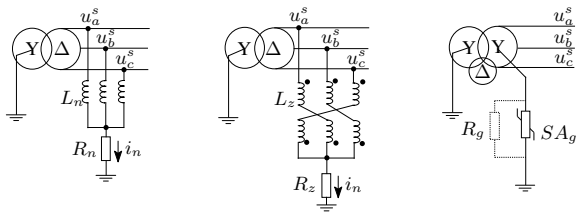

Figure 5. AC side grounding potential candidates (a) Star point reactor (b) Zig-zag transformer (c) Yyd transformer with a fixed or non-linear grounding resistor.

the DC bus/line surge arresters, and have comparatively lower switching impulse protective levels to intentionally provide a discharge path for the healthy pole.

AC side groundings can be divided into two types based on the converter transformer configuration: (1) Yd transformer with additional grounding equipment, such as a star point reactor or a zig-zag grounding transformer [16], [20], and (2) Dy transformer with its neutral grounded with a fixed or non-linear resistor [13]. Since ungrounded primary side is not typically used for HVDC applications, a Yy transformer with tertiary delta (Fig. 5 (c)) is a possible solution to utilize a neutral grounded resistor [21]. These AC groundings provide a zero sequence path to the DC side while preventing zero sequence from entering the connected AC system, which means the zero sequence current only flows in the AC grounding.

$$u_0^s = Z_0^{gnd} i_0^{\Delta}, \tag{7}$$

where Z_0^{gnd} is the zero sequence impedance of the AC grounding.

$$Z_0^{gnd} = \begin{cases} sL_n + 3R_n, \text{star point reactor} \\ sL_z + 3R_z, \text{zig-zag transformer} \\ sL_y + 3R_g, \text{Yyd transformer,} \end{cases} \tag{8}$$

and L_z and L_y is the leakage inductance of the zig-zag and Yyd transformer, respectively. Substituting (7) into (5), gives

$$\frac{u_{DCp} - u_{DCn}}{2} + u_0^{\Delta} = (\frac{sL_{arm}}{2} + Z_0^{gnd}) i_0^{\Delta}. \tag{9}$$

Therefore, the voltage imbalance between the two poles drives a zero sequence current in the AC grounding.

The behaviour of the pole rebalancing equipment can be divided into three stages: normal operation, before fault clearing, and after fault clearing.

1) During normal operation: the DBS is turned off, and consequently, consumes no power during normal operation. On the contrary, the AC grounding consumes apparent power due to a positive sequence current, and a zero sequence current if a third harmonic injection is used for modulation. The apparent power consumption consists of positive and zero sequence for the star point reactor (S_s) and the zig-zag transformer (S_z), but only zero sequence for the neutral grounded Yyd transformer (S_y). The apparent power is calculated as

$$\begin{cases} S_s = \dfrac{(U_1^s)^2}{\omega_1 L_n} + \dfrac{(U_0^s)^2}{\sqrt{(3\omega_1 L_n)^2 + (3R_n)^2}} \\ S_z = \dfrac{(U_1^s)^2}{\omega_1 L_z + 3I_1/I_0(\omega_1 L_z)} + \dfrac{(U_0^s)^2}{\sqrt{(3\omega_1 L_z)^2 + (3R_z)^2}} \\ S_y = \dfrac{(U_0^s)^2}{\sqrt{(3\omega_1 L_y)^2 + (3R_g)^2}}, \end{cases} \tag{10}$$

where ω_1 is the fundamental frequency; I_1, I_0 is the rated current and magnetizing current of the zig-zag transformer; U_1^s and U_0^s is the positive and zero sequence line-to-line RMS voltage.

Controllable switches can be used to actively reduce or eliminate the apparent power consumptions of the AC groundings. Example circuits are proposed in Fig. 6. These switches are in open position during normal operation, and do not require current interrupting capability. Therefore, fast making switches such as thyristor-based switches or high speed making switches are considered applicable for this application [22], [23]. The closing time ($t_{br,c}$) of thyristor-based switches and high speed mechanical making switches is in the order of 1 ms and 10 ms, respectively [22], [23].

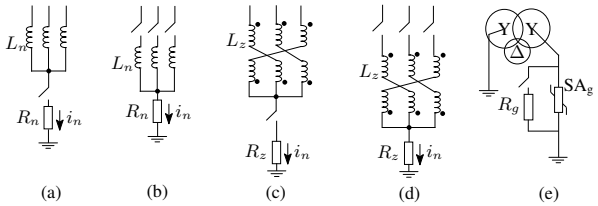

Figure 6. AC side grounding options with controllable switches.

2) Before fault clearing: The equivalent circuit given in Fig. 3 (b) shows that an additional fault current path is formed by the AC groundings, without using controllable switches. Similarly, Fig. 2 (b) clearly depicts a pole-to-pole path formed via the DBS, if typical DBS control for offshore wind application is applied. These additional paths contribute to the fault current experienced by the DC circuit breaker and the converter. Therefore, the impedance of the pole rebalancing equipment — fixed or non-linear resistance of a DBS and zero sequence impedance Z_0^{gnd} of a AC grounding — should be dimensioned appropriately to avoid increasing the breaking current requirement.

3) After fault clearing: After fault clearing, the DBS or the AC grounding is controlled to provide a discharge path for the healthy pole to restore normal pole voltages. The main design parameter dictating the pole rebalancing performance is the impedance of the pole rebalancing equipment. The choice of the impedance is a trade-off between achieving high pole rebalancing speed and limiting currents in the discharge path.

III. Proposed Pole Rebalancing Controls

A. DBS Controller

The proposed DBS controller is designed to avoid adverse interactions with the DC circuit breaker in creating a pole-to-pole path. To avoid such path, the DBS controller needs to be aware of the fault clearing instant to delay the DBS operation. Various methods can be used to estimate the fault clearing instant, such as estimating the fault clearing using breaker opening time, communicating the breaker status after breaker tripping. The proposed DBS controller is shown in Fig. 7. The DBS switches are controlled by monitoring the pole overvoltage or pole voltage imbalance. The fault clearing instant is estimated by communicating the tripping command to the DBS controller, and the DBS operation is delayed for the anticipated breaker opening time ($t_{br,o}$) with an additional 1 ms margin. An enable/disable signal EN_{com} is included to demonstrate the impact of delaying the DBS operation.

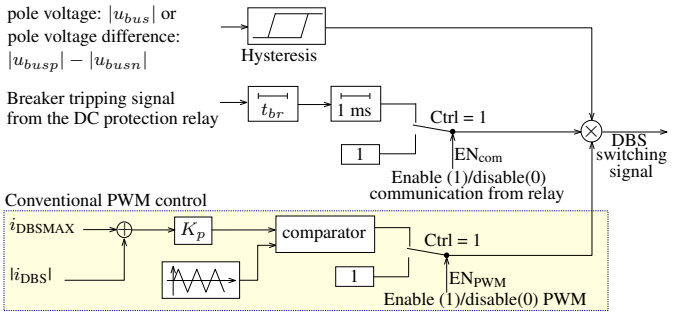

Figure 7. Schematic diagram of the DBS controller.

As comparison, a typical DBS controller for offshore wind application is implemented, in which the insulated-gate bipolar transistor (IGBT) switches are controlled by pulse width modulation (PWM) to regulate the dissipated energy in the braking resistor, adopting a similar control methodology as described in [17]. PWM switching might not be applicable for pole rebalancing due to switching transients. In a point-to-point link, the DBS is typically placed between the DC smoothing reactor and the cable, such that the switching transients are largely mitigated by the stray capacitance of the cable. However, in an HVDC grid (Fig. 2), the DBS is likely to be directly connected to the busbar between the DC smoothing reactor and the series line inductors. Chopping these inductive currents causes high voltage stress on the IGBT switches and the DC cables.

B. Zero Sequence Current Controller for AC Grounding

To avoid oscillations during pole rebalancing, a zero sequence current controller is designed to smoothly rebalance poles based on (9). The block diagram of the zero sequence current controller is given in Fig. 8. The measured zero sequence current i_0^{Δ} is regulated by a proportional integral (PI) controller to follow the reference $i_0^{\Delta *}$, set as zero. The output of the zero sequence current controller gives the zero sequence differential-mode voltage reference $u_0^{\Delta *}$. This reference is added to calculate the arm voltage references u_ϕ^{U*} and u_ϕ^{L*} using (11) and (12). The zero sequence controller is always activated, and no additional triggering is necessary for fault conditions.

$$u_\phi^{U*} = \frac{U_{DC}}{2} - u_\phi^* - u_0^{\Delta *} \tag{11}$$

$$u_\phi^{L*} = \frac{U_{DC}}{2} + u_\phi^* + u_0^{\Delta *} \tag{12}$$

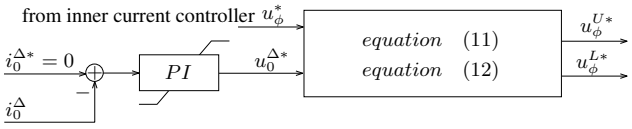

Figure 8. Block Diagram of the zero sequence current controller.

If controllable switches are used for AC groundings, they are commanded to close once a pole-to-ground fault is detected by the DC relay.

IV. Test System

A. Four-terminal HVDC Grid

The test system, shown in Fig. 9, is developed based on the model provided in [24]. The converters are of the half-bridge based MMC type. The converter model, control and internal protection are adapted from [24] to match a rated power of 1265 MVA. The converter transformer is a two-winding Yd transformer with ungrounded delta connection at the valve side. DC line and DC bus surge arresters are implemented to provide overvoltage protection. AC side surge arresters are not considered in this study. The same U-I characteristics taken from [25] are used for all surge arresters. The main parameters of the test system are given in Table I.

The DBS and AC groundings are implemented at the two onshore stations: MMC1 and MMC3. For each study, only one of the options, DBS or AC grounding, is activated. The breaker opening time and the series inductor are 20 ms and

50 mH unless stated otherwise. A solid pole-to-ground fault (f_1) is applied at the positive terminal of cable L_{13}. This study considers local measurement based fault protection algorithms, which have a fault detection time in the order of few hundreds of microseconds [26], [27]. The fault detection is emulated using a fixed time delay of 0.5 ms after the fault initiated travelling wave arrives at the relay position.

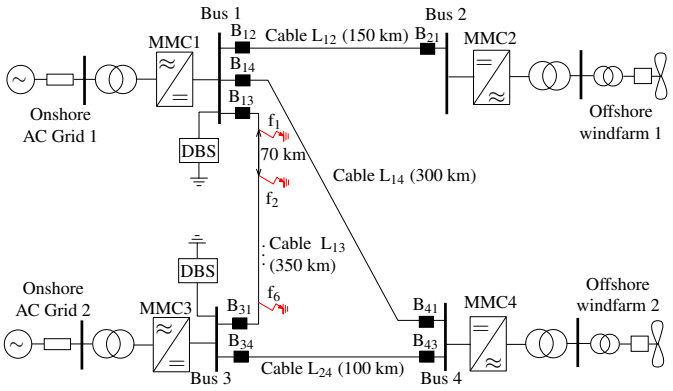

Figure 9. A four-terminal symmetrical monopolar test system.

Table I
CONVERTER AND GRID PARAMETERS

Parameters	Symbol	Value	Unit
Rated apparent power	S	1265	[MVA]
Rated active power	P_{DC}	1200	[MW]
Rated DC pole-to-ground voltage	U_{DCp}, U_{DCn}	±320	[kV]
Rated transformer voltages	U_{AC1}/U_{AC2}	400/333	[kV]
Transformer leakage impedance	μ_k	0.18	pu
Arm capacitance	C_{arm}	22	[μF]
Arm inductance	L_{arm}	42	[mH]
Arm resistance	R_{arm}	0.6244	[Ω]
DC smoothing reactor	L_{DC}	10	[mH]
Line inductor	L_{line}	10 ∼ 100	[mH]

B. DBS Model and Controller

Similar to point-to-point offshore wind applications, the braking resistor R_{DBS} is rated for the nominal power of a single MMC [17].

$$R_{\text{DBS}} = \frac{U_{DC}^2}{2 \cdot P_{DC}} \tag{13}$$

where R_{DBS} is the braking resistance per pole, U_{DC} is the rated DC pole-to-pole voltage, and P_{DC} is the rated active power of a single MMC.

The reference voltage of the surge arresters, SA_{DBSa} and SA_{DBSb1} are chosen to have a switching impulse protection level of 1.2 pu as suggested in [19]. A proportional current controller using PWM switching is implemented to investigate the switching transients. Parameters of the DBS controller are listed in Table II.

C. Dimension of AC Groundings

As a trade-off of apparent power consumption and pole rebalancing speed, the zig-zag transformer is rated at 3 MVA.

Table II
MAIN PARAMETERS OF THE DBS CONTROLLER

Maximum reference current I_{DBSMAX}	2	[kA]
Proportional control gain K_p	0.5	
Hysteresis HI/LO	1.1/1.05	[pu]
PWM frequency	2	[kHz]

The voltage rating is 333 kV at the valve side. The excitation current is 1% of the nominal load current and the leakage impedance is 0.1 pu. The neutral resistor R_z is chosen as 200 Ω to have sufficient damping. The positive sequence and the total apparent power consumption is 0.1 MVA and 0.32 MVA, respectively, considering 15% of third harmonic injection.

The star point reactor and the grounding resistance of the Yyd transformer are chosen to produce the same on-state apparent power consumption as the zig-zag transformer using (10), which gives L_n = 1096 H and R_g = 2564 Ω. The inductance L_n is considered realistic since the inductance of star point reactors used for grounding is typically in the range of 5000 H [28]. The protection level of the neutral grounding surge arrester is chosen taking into consideration both reducing insulation cost and avoiding high current during pole-to-ground faults.

D. Pole-to-ground Fault Response

An example of the pole-to-ground fault response is given in Fig. 10, considering three inductor sizes and six fault locations indicated in the test grid. The DC line and bus surge arresters are put out of service in these simulations to show the prospective system response without protection. The fault current shows a damped oscillation through the arm resistance and inductance with large amplitudes due to cable and MMC submodule capacitors discharge. If fast breakers are only dimensioned for pole-to-ground faults, high interruption capabilities are still needed. However, if slow DC circuit breakers (≈ 20 ms) are used, the requirement is only a few kA, regardless of the series inductor size and fault location. The trade-off of employing slow DC circuit breakers is the complete discharge of the faulted pole, which imposes larger duties to the pole rebalancing equipment and DC side surge arresters, and higher overvoltage stress to the healthy pole cables. Moreover, fast DC circuit breakers can also interrupt pole-to-pole faults; whereas such faults need to be handled by other protective devices such as AC breakers, if slow breakers with low breaking current capability are utilized.

V. CASE STUDIES

A. DBS Performance

1) Applicability of DBS circuit 1: The requirements on the DBS for pole rebalancing differ with those for point-to-point offshore wind application mainly in two aspects, as shown in Fig. 11. First, switching off the DBS causes high voltage stress on the DC bus and the IGBT switches due to the switching of inductive current. These switching transients are more pronounced with PWM control. Therefore,

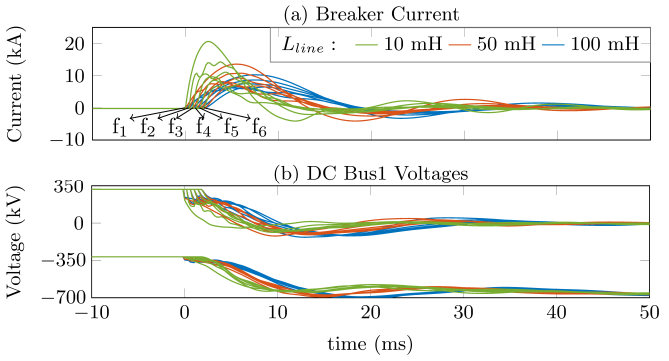

Figure 10. Fault current in B_{13} and bus voltage during pole-to-ground faults (fault location: f_1 to f_6 distributed on a 350 km cable with a 70 km internal, DC line/bus surge arresters out of service).

hysteresis control without PWM switching is preferable from the perspective of reducing voltage transients. Furthermore, the insulation level of the total IGBT stack needs to be dimensioned for higher voltage (Fig. 11 (d)) for this DBS circuit regardless of PWM switching, unless an additional voltage limiting device is installed for the IGBT stack. Second, the required energy absorption capability is much smaller for pole rebalancing compared with that for offshore wind application. The dissipated energy in the DBS without PWM switching at MMC1 and MMC3 is 38.3 MJ and 50.2 MJ, which results in a total energy requirement of 88.6 MJ. In offshore applications, the DBS is typically dimensioned to absorb the full capacity for a few hundred ms during an onshore AC fault, resulting in energy requirement in the range of a few hundred MJ [17].

Compared to the base case without DBS, the current in B_{13p} is slightly larger with the DBS in operation. The pole rebalancing time, defined as the time period from fault inception to the instant when the pole voltage returns within the normal range ([0.95 $\sim$ 1.05 pu]), is 67 ms and 64 ms for the case with and without PWM switching, respectively.

In conclusion, the DBS implementation as used in existing offshore application cannot be directly used for pole rebalancing in a selective protection strategy due to the required insulation level of the IGBT.

2) Performance of DBS circuit 2 and 3: Unlike the resistor based DBS, the surge arrester based DBS circuits are suitable for pole rebalancing application thanks to the non-linear resistors and the proposed controller. The voltage transients observed when switching off the DBS are negligible (Fig. 12 (b) and (d)) since the surge arrester only allows for small currents under low voltage. Consequently, the insulation level of the IGBT stack can be dimensioned for pole-to-ground voltage for these two DBS circuits, which is more cost effective in comparison with that of the resistor based DBS. The pole rebalancing time is approximately 80 ms using surge arrester based DBS circuits regardless of the delay in the DBS operation.

The proposed control strategy reduces the breaking current and energy of the DC circuit breaker, and the required energy absorption capability of the DBS by delaying the

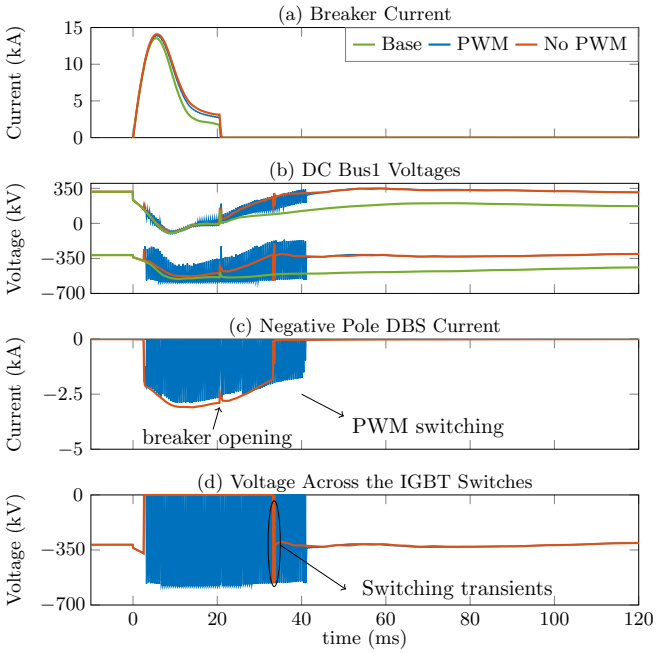

Figure 11. Impact of PWM switching using DBS circuit 1 for pole rebalancing. Base: reference case without DBS; PWM/No PWM: with/without PWM switching.

DBS operation. The required breaking current is 1.9 kA and 8.2 kA with/without delaying the DBS operation. The dissipated energy in the two DBS can be reduced from 115 MJ to 33 MJ by delaying the DBS operation after breaker opening.

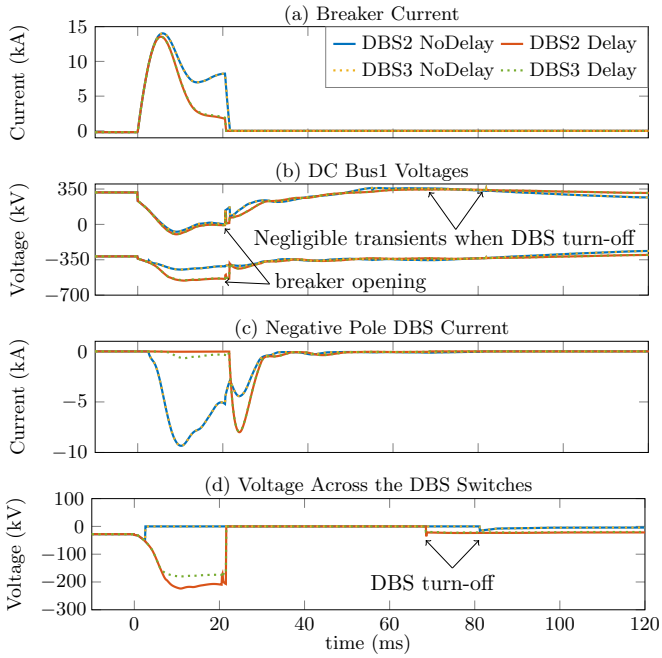

Figure 12. Performance of DBS circuit 2 and 3. DBS2 NoDelay/DBS3 NoDelay: operate DBS circuit 2/3 upon detecting voltage imbalance; DBS2 Delay/DBS3 Delay: delay operation of DBS circuit 2/3.

B. AC Grounding Performance

1) Impact of the zero sequence current control: The proposed zero sequence current control achieves faster pole rebalancing compared with uncontrolled rebalancing through damping the oscillations which would result otherwise (Fig. 13 (b)). The proposed controller also reduces the dissipated energy from 12 MJ to 3 MJ. The zero sequence current control causes voltage divergence between the upper and lower arm capacitors since a zero sequence voltage of the opposite sign is added to the reference arm voltages to control the zero sequence current. The peak sum capacitor voltages of the upper arms are increased from 1.24 pu to 1.28 pu with the zero sequence current control in operation (Fig. 13 (c)). A grounding resistor of 200 Ω should not increase the voltage rating of the submodules considering that they are dimensioned to withstand 1.3 pu overvoltage during an AC single-phase-to-ground fault [29].

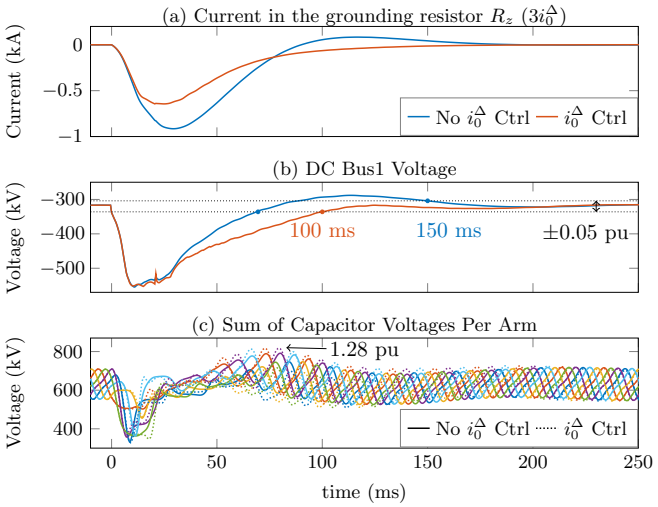

Figure 13. Impact of zero sequence current control using zig-zag transformer. No i_0^Δ Ctrl/i_0^Δ Ctrl: zero sequence current control not in operation/in operation.

2) Performance considering the same apparent power consumption: The performance of a star point reactor depends on the total zero sequence impedance and the ratio between the inductance L_n and the resistance R_n. Three R_n/L_n ratios, 0, 1, and 2 are tested, keeping the inductance L_n fixed at 1096 H. A large grounding resistor reduces the overshoot in the DC voltage by providing more damping and consequently reduces pole rebalancing time as shown in Fig. 14. Under the same apparent power consumption condition as a zig-zag transformer, the pole rebalancing time with a star point reactor and a neutral grounded Yyd transformer is 436 ms and 690 ms, respectively.

3) Impact of dimension and active switching: The pole rebalancing time can be reduced by decreasing the zero sequence impedance of the AC groundings, at the cost of increased apparent power consumption. To achieve similar pole rebalancing speed as the zig-zag transformer, the inductance L_n and parallel resistor R_g of the star point reactor and the Yyd transformer has to be in the range of 50 H and 220 Ω,

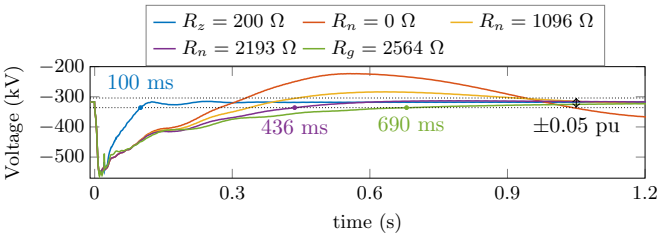

Figure 14. Comparison of pole rebalancing times of zig-zag transformer, star point reactor and neutral grounded YY transfer considering the same apparent power consumption.

respectively. The apparent power consumption increases to 7.11 MVA and 3.78 MVA.

Three phase or neutral switches are capable of reducing or eliminating the apparent power consumptions of the AC groundings. Apparent power consumption comparison with and without using active switching is given in Table III. The closing time of the controllable switches is simulated as 20 ms for the reference cases, shown in Fig. 15. These switches have to withstand the AC or neutral voltages during DC faults as shown in Fig. 15 (b).

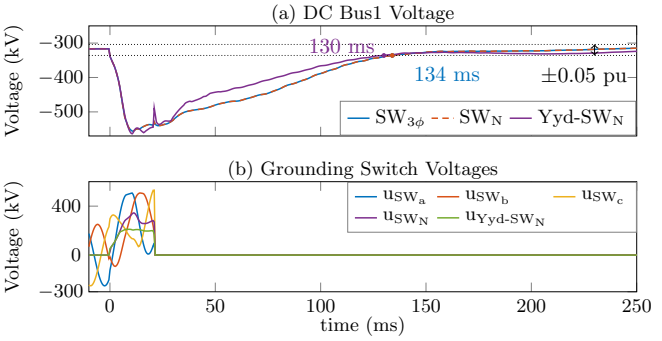

Figure 15. Impact of using active switching for AC groundings. $SW_{3\phi}$, SW_N: star point reactor using three phase or neutral switches; Yyd-SW_N: Yyd transformer using neutral switch.

Table III
APPARENT POWER CONSUMPTIONS AND POLE REBALANCING SPEED OF AC GROUNDINGS ($t_{br,c}$ = 20 MS)

AC Groundings		Apparent Power Consumption [MVA]	Speed [ms]
Star point reactor	Without switches	7.11	122
	Neutral point switch	7.06	134
	Three phase switches	0	134
Zig-zag transformer	Without switches	0.32	100
	Neutral point switch	0.1	112
	Three phase switches	0	112
Neutral grounded Yyd transformer	Without switches	3.78	130
	Neutral point switch	0	130

The impact of the closing time $t_{br,c}$ on the pole rebalancing performance is investigated using a three phase switch with star point reactors, by varying $t_{br,c}$ from 1 ms up to 50 ms. The upper value of 50 ms is considered here since high speed earthing switches with such closing speed have already been

installed in existing HVDC links [5]. Fig. 16 and Fig. 17 show that slower closing time results in longer pole rebalancing time, but will not significantly increase the required energy absorption capability of the relevant DC surge arresters. The required closing speed of the active switches is thus mainly determined by the expected pole rebalancing speed. A closing time less than 20 ms gives comparable pole rebalancing speed as a zig-zag transformer.

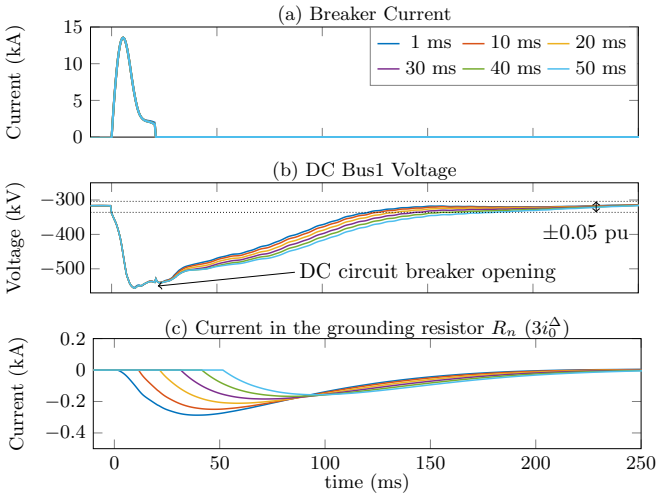

Figure 16. Impact of closing time, $t_{br,c}$ of the active switches on pole rebalancing performance.

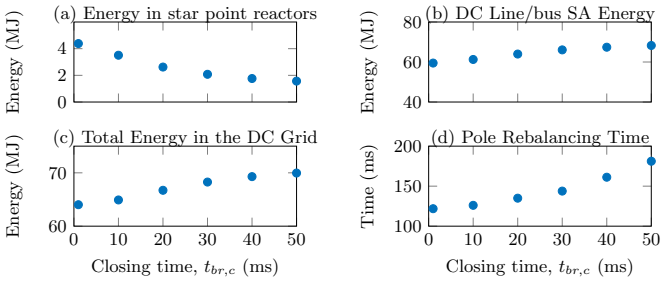

Figure 17. Impact of closing time, $t_{br,c}$ of the active switches on pole rebalancing performance.

4) Summary: A zig-zag transformer combined with zero sequence current control can achieve comparable speed as the surge arrester based DBS for pole rebalancing with only marginal apparent power consumption. The zero sequence current control is capable of speeding up the pole rebalancing process through increased damping of the zero sequence current. For the same apparent power consumption as the zig-zag transformer, the star point reactor and neutral grounded Yyd transformer requires a few hundreds of ms to rebalance the pole. Star point reactor and neutral grounded Yyd transformer can achieve comparable rebalancing speed using additional controllable switches, otherwise the power consumptions are considered too high for practical application.

C. Interaction between DC circuit breaker requirements on pole rebalancing requirements

This section investigates the link between breaker requirements and pole rebalancing needs introduced by different breaker technologies. The two parameters essential in this analysis are the breaker opening time and the required series inductor size. In particular, this section investigates the influence of the breaker parameters on the breaking current requirement, pole rebalancing speed and required energy absorption capability of the whole DC grid including DC circuit breakers, DC bus/line surge arresters and the pole rebalancing equipment.

1) Breaker opening time: The breaker opening time is varied from 0.5 ms to 20 ms with a 0.5 ms interval and the series inductor is fixed at 50 mH.

As shown in Fig. 18 (a) and (b), the breaker current and energy does not linearly increase as the breaker opening time increases. A breaker opening time of about 5 ms results in the highest breaking current and energy requirement.

Delaying the DBS operation is the most beneficial for breakers with opening time larger than 5 ms. Delaying the DBS operation has insignificant impact on the pole rebalancing times. However, it largely reduces breaking current and energy of the breaker and reduces the required energy absorption capability of the DBS and the whole grid.

The pole rebalancing time is insensitive to the breaker opening time, with reduced time only when a very fast breaker is used. The pole rebalancing time is about 100 ms for both the DBS and zig-zag transformer (Fig. 18 (f)).

The advantage of the zig-zag transformer is a low requirement in terms of energy absorption capability. The energy dissipated in the zig-zag transformers is only a few MJ, which is one order less compared to the DBS.

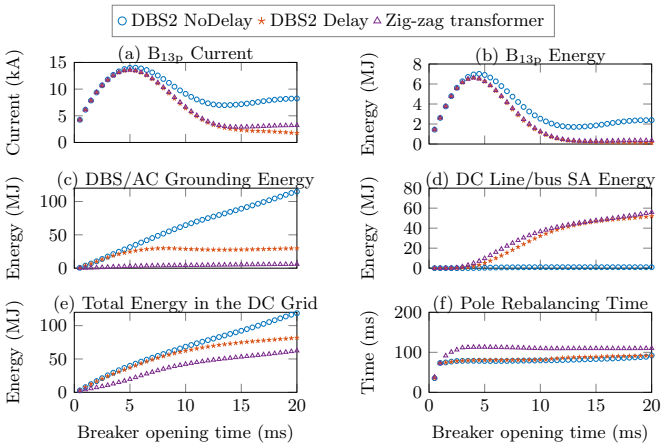

Figure 18. Impact of DC circuit breaker opening time, $t_{br,o}$

2) Series line inductor: Two breaker opening times, 2 ms and 20 ms are considered in this study. The inductors are varied from 10 mH to 200 mH with a 10 mH interval.

As shown in Fig. 19, it is more advantageous to use a larger inductor for a 2 ms DC circuit breaker to reduce the requirement on the breaker current and energy. The total

dissipated energy in the whole grid also decreases as the series inductor increases.

As shown in Fig. 20, for a breaker with 20 ms opening time, it is more advantageous to operate the DBS after breaker opening, which results less current and energy of the DC circuit breaker and less total dissipated energy in the whole grid. The size of the inductor has less influence and therefore a small inductor is preferred in this case.

In general, zig-zag transformers give better performance in terms of the required energy absorption capability; whereas the DBS gives slightly better performance in pole rebalancing speed and has zero apparent power consumption during normal operation.

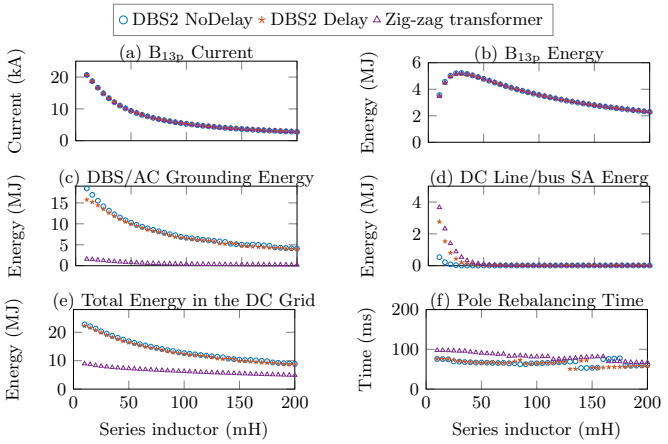

Figure 19. Impact of series inductor size, L_{line} (DC circuit breaker opening time, $t_{br,o}$ = 2 ms).

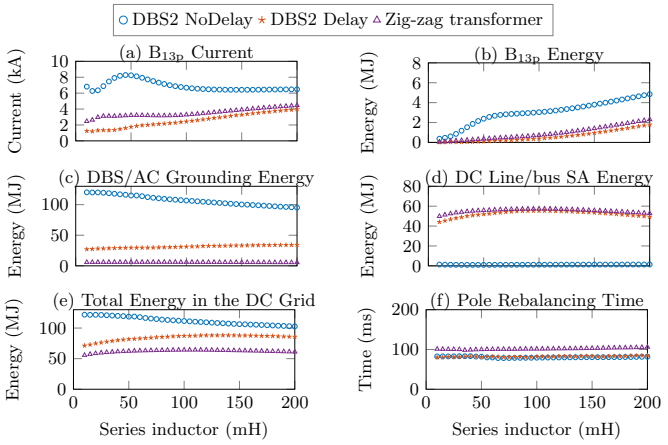

Figure 20. Impact of series inductor size, L_{line} (DC circuit breaker opening time, $t_{br,o}$ = 20 ms).

VI. Conclusion

Pole rebalancing in HVDC grids employing DC circuit breakers requires control during three stages: before, during and after fault clearing. The pole rebalancing methods and controls proposed in this paper provide low losses and high speed of pole rebalancing, which are essential in selectively protected HVDC grids.

Before breaker opening, uncoordinated DBS operation leads to unwanted high fault current, which is avoided by the proposed control method. The AC groundings face a trade-off between apparent power consumption and pole rebalancing speed. Proper dimensioning of the AC groundings and utilizing controllable switches could allow high speed pole rebalancing with reduced apparent power consumption. In addition, alternative pole rebalancing circuits at both AC and DC sides are investigated in this paper. The main advantage of the DBS is zero apparent power consumption, whereas the AC groundings require less energy absorption capability.

Finally, interaction studies of DC circuit breakers and pole rebalancing equipment demonstrate the trade-off in speed of fault clearing versus requirements on pole rebalancing equipment and DC side surge arresters. Use of fast DC circuit breaker reduces the requirements on pole rebalancing and DC side surge arresters; however, the required interruption and energy absorption capability of the DC circuit breakers are high. On the contrary, waiting until the fault current decreases to a low value reduces the required interruption capability of DC circuit breakers, but increases the required energy absorption capability of the pole rebalancing equipment and DC side surge arresters. Coordinating the DBS operation is more advantageous to reduce the breaker requirements and the required total energy absorption capability when using with slow DC circuit breakers.

References

[1] D. Van Hertem and M. Ghandhari, "Multi-terminal VSC HVDC for the European supergrid: Obstacles," *Renewable and Sustainable Energy Reviews*, vol. 14, no. 9, pp. 3156–3163, Dec. 2010.

[2] W. Leterme and D. Van Hertem, "Classification of Fault Clearing Strategies for HVDC Grids," in *Proc. Cigré Lund Symp.*, Lund, Sweden, 27–28 May 2015, 10 pages.

[3] J. Häfner and B. Jacobson, "Proactive Hybrid HVDC Breakers - a key innovation for reliable HVDC grids," in *Proc. Cigré Bologna Symp.*, Bologna, Italy, 13–15 Sept. 2011, 8 pages.

[4] K. Tahata, S. El Oukaili, K. Kamei, D. Yoshida, Y. Kono, R. Yamamoto, and H. Ito, "HVDC circuit breakers for HVDC grid applications," in *Proc. AORC-cigré 2014*, Tokyo, Japan, 27–29 May 2014, 9 pages.

[5] Cigré Joint Working Group A3-B4.34, "Technical Requirements and Specifications of State-of-the-art HVDC Switching Equipment," *Cigré Technical Brochure*, 2017.

[6] M. Wang, M. Abedrabbo, W. Leterme, D. Van Hertem, C. Spallarossa, S. Oukaili, I. Grammatikos, and K. Kuroda, "A Review on AC and DC Protection Equipment and Technologies : Towards Multivendor Solution," in *Proc. Cigré 2017 Canada*, Winnipeg, Canada, 30 Sep. - 6 Oct. 2017, 11 pages.

[7] O. Cwikowski, A. Wood, A. Miller, M. Barnes, and R. Shuttleworth, "Operating DC Circuit Breakers with MMC," *IEEE Trans. Power Del.*, vol. 33, no. 1, pp. 260–270, 2017.

[8] R. Li, L. Xu, D. Holliday, F. Page, S. Finney, and B. Williams, "Continuous Operation of Radial Multi-terminal HVDC Systems under DC Fault," *IEEE Trans. Power Del.*, vol. 31, no. 1, pp. 351–361, 2016.

[9] N. A. Belda, C. Plet, and R. P. Smeets, "Analysis of Faults in Multi Terminal HVDC Grid for Definition of Test Requirements of HVDC Circuit Breakers," *IEEE Trans. Power Del.*, vol. 33, no. 1, pp. 403–411, 2017.

[10] O. Cwikowski, H. Wickramasinghe, G. Konstantinou, J. Pou, M. Barnes, and R. Shuttleworth, "Modular Multilevel Converter DC Fault Protection," *IEEE Trans. Power Del.*, vol. 33, no. 1, pp. 291–300, 2017.

[11] PROMOTioN WP 4, "D4.1 Definition of test cases and functional requirements for DC grid protection methodologies," Tech. Rep., Feb. 2017.

[12] G. Chaffey and T. C. Green, "Low speed protection methodology for a symmetrical monopolar HVDC network," in *Proc. IET ACDC 2017*, Manchester, UK, 14–16, Feb. 2017, 6 pages.

[13] L. Tang, "Control and Protection of Multi-Terminal DC Transmission Systems Based on Voltage-Source Converters," Ph.D. dissertation, McGill University, Montreal, Quebec, Canada, 2003.
[14] P. Mitra, J. Hanning, J. Kohlstrom, T. Larsson, and J. Danielsson, "DC grid system behavior: A real-time case study," in *2015 IEEE PES GM*, Denver, U.S., 26–30, July 2015, 5 pages.
[15] L. Harnefors, A. Antonopoulos, S. Norrga, L. Ängquist, and H. P. Nee, "Dynamic Analysis of Modular Multilevel Converters," *IEEE Trans. Ind. Electron.*, vol. 60, no. 7, pp. 2526 – 2537, 2013.
[16] A. Junyent-Ferré, P. Clemow, M. M. C. Merlin, and T. C. Green, "Operation of HVDC modular multilevel converters under DC pole imbalances," in *Proc. EPE-ECCE 2014*, Lappeenranta, Finland, 26–28 Aug. 2014, 10 pages.
[17] J. Maneiro, S. Tennakoon, C. Barker, and F. Hassan, "Energy diverting converter topologies for HVDC transmission systems," in *Proc. EPE-ECCE 2013*, Lille, France, 2-6 Sept. 2013, 10 pages.
[18] J. Nunes and J. Karlsson, "Method and a device for overvoltage protection, and an electric system with such a device," US 2004 / 0180361A1, 30 Aug. 2012, 10 pages.
[19] L.-E. Juhlin, "Voltage balancing of symmetric HVDC monopole transmission lines after earth faults," U.S. Patent US 2013/0229739 A1, 5 Sept. 2013, 12 pages.
[20] H. Wang, G. Tang, Z. He, and J. Yang, "Efficient grounding for modular multilevel HVDC converters (MMC) on the AC side," *IEEE Trans. Power Del.*, vol. 29, no. 3, pp. 1262–1272, 2014.
[21] A. Alefragkis, S. M. I. Huq, P. Weitzenfelder, and R. T. Pinto, "Design Considerations for the extension of COBRAcable point-to-point HVDC transmission link into a Multi-terminal system," in *Proc. Cigré 2017*, Winnipeg, Canada, 30 Sep. - 6 Oct. 2017, 8 pages.
[22] A. A. Elserougi, A. S. Abdel-Khalik, A. M. Massoud, and S. Ahmed, "A new protection scheme for hvdc converters against dc-side faults with current suppression capability," *IEEE Trans. Power Del.*, vol. 29, no. 4, pp. 1569–1577, Aug. 2014.
[23] Promotion WP 6, "D6.2 Develop system level model for mechanical DCCB," Dec. 2016. [Online]. Available: https://www.promotion-offshore.net/fileadmin/PDFs/D6.2_PROMOTioN_Deliverable_Develop_system_level_model_for_mechanical.pdf
[24] N. Ahmed, L. Angquist, S. Mehmood, A. Antonopoulos, L. Harnefors, S. Norrga, and H.-P. Nee, "Efficient Modeling of an MMC-Based Multiterminal DC System Employing Hybrid HVDC Breakers," *IEEE Trans. Power Del.*, vol. 30, no. 4, pp. 1792–1801, 2015.
[25] F. B. Ajaei and R. Iravani, "Cable Surge Arrester Operation Due to Transient Overvoltages Under DC-Side Faults in the MMC-HVDC Link," *IEEE Trans. Power Del.*, vol. 31, no. 3, pp. 1213–1222, June 2016.
[26] W. Leterme, J. Beerten, and D. Van Hertem, "Non-unit protection of HVDC grids with inductive dc cable termination," *IEEE Trans. Power Del.*, vol. 31, no. 2, pp. 820–828, Apr. 2016.
[27] J. Sneath and A. D. Rajapakse, "Fault detection and interruption in an earthed HVDC grid using ROCOV and hybrid DC breakers," *IEEE Trans. Power Del.*, vol. 31, no. 3, pp. 973–981, June 2016.
[28] S. Dennetière, S. Nguefeu, H. Saad, and J. Mahseredjian, "Modeling of modular multilevel converters for the France-Spain link," in *Proc. IPST*, Vancouver, Canada, 18–20 July 2013, 7 pages.
[29] K. Sharifabadi, L. Harnefors, H.-P. Nee, R. Teodorescu, and S. Norrga, *Design, Control and Application of Modular Multilevel Converters for HVDC Transmission Systems*. John Wiley & Sons, 2016.

Mian Wang (S'16) received the M.Eng. degree in electrical engineering from Kyoto University in 2011. She worked as a Power System Engineer in Power and Industrial Systems R&D Centre Toshiba from 2011 to 2015. Currently, she is pursuing her Ph.D. in the department of Electrical Engineering at KU Leuven/EnergyVille. Her research interests are high voltage DC Transmission, multivendor DC grid protection systems.

Willem Leterme (S'12,M'16) received the M.Sc. and Ph.D. degree in electrical energy engineering from KU Leuven, Belgium, in 2012 and 2016. Currently, he is a postdoctoral researcher at KU Leuven/EnergyVille. His research interests are in the area of power system protection, in which he focuses on protection of multi-terminal and meshed VSC HVDC systems.

Geraint Chaffey (S'13) received the M.Eng. degree in electrical and electronic engineering from Cardiff University, Cardiff, U.K., in 2012, and the Ph.D. degree from Imperial College London, London, U.K., in 2017. His doctoral thesis was titled "The Impact of Fault Blocking Converters on HVDC Protection." He is currently a Postdoctoral Researcher with KU Leuven/EnergyVille, where his current research interests include HVDC protection and the impact on connected AC systems.

Jef Beerten (S'07-M'13) received the M.Sc. degree in electrical engineering and the Ph.D. degree from the University of Leuven (KU Leuven), Belgium, in 2008 and 2013, respectively.
Currently, he is an Assistant Professor with KU Leuven/EnergyVille. His research interests include power system dynamics and control and the impact of HVDC systems in particular. Dr. Beerten is an active member of both the IEEE and CIGRÉ.

Dirk Van Hertem (S'02,SM'09) received the Ph.D. degree from KU Leuven, Belgium, in 2009. In 2010, he was a member of EPS group at the Royal Institute of Technology, Stockholm, Sweden. He is an Associate Professor at KU Leuven, Belgium. His fields of interest are power system operation and control in systems with FACTS and HVDC and the transmission system of the future, including offshore grids and the supergrid. He is an active member of IEEE PES, IAS and CIGRÉ.